

Functionalization of Coordination Nanochannels for Controlling Tacticity in Radical Vinyl Polymerization

Takashi Uemura,^{*,†,‡} Yukari Ono,[†] Yuh Hijikata,[†] and Susumu Kitagawa^{*,†,‡,§}

Department of Synthetic Chemistry and Biological Chemistry, Graduate School of Engineering, Kyoto University, Katsura, Nishikyo-ku, Kyoto 615-8510, Japan, PRESTO, Japan Science and Technology Agency (JST), Kawaguchi, Saitama 332-0012, Japan, and Institute for Integrated Cell-Material Sciences (iCeMS), Kyoto University, Yoshida, Sakyo-ku, Kyoto 606-8501, Japan

Received January 15, 2010; E-mail: uemura@sbchem.kyoto-u.ac.jp; kitagawa@sbchem.kyoto-u.ac.jp

Abstract: Systematic functionalization of porous coordination polymers (PCPs), $[\text{Cu}_2(\text{L})_2(\text{ted})]_n$ (where L = dicarboxylates and ted = triethylenediamine), by introducing various substituents onto the component organic ligand, L, was performed to regulate the radical polymerization of methyl methacrylate (MMA) in the nanochannels. The effect of the substituent groups on stereoregularity of the resulting poly(methyl methacrylate) (PMMA) was observed, where the tacticity of the PMMA strongly depended on the number and position of the substituent. In particular, polymerization of MMA in $[\text{Cu}_2(2,5\text{-dimethoxyterephthalate})_2(\text{ted})]_n$ gave PMMA with high isotactic and heterotactic triad fractions, which is one of the most effective systems for changing the tacticity of PMMA in radical polymerization. To understand the mechanism of this drastic stereoregularity change, a variety of experimental and theoretical analyses, such as IR, N_2 adsorption, a statics study, and molecular dynamics (MD) calculations, were performed. Accurate MD calculations were helpful to determine the most plausible structures of $[\text{Cu}_2(\text{L})_2(\text{ted})]_n$ and revealed that the specific channel shape of $[\text{Cu}_2(2,5\text{-dimethoxyterephthalate})_2(\text{ted})]_n$ induces the large tacticity change of the resulting PMMA.

Introduction

In recent years, there has been considerable interest in porous coordination polymers (PCPs) or metal–organic frameworks (MOFs) composed of transition metal ions and bridging organic ligands.¹ In this research area, the structural versatility of molecular chemistry has allowed the rational design and assembly of materials with novel topologies and exceptional host–guest properties. Thus, PCPs have emerged as a particular class of functional solid materials for applications in many areas, including storage, separation, and exchange.¹ An especially notable characteristic of PCPs is their regular nanochannels that can be utilized for catalysts and molecular reactions.² Well-defined nanochannel structures based on PCPs have potential advantages for inducing highly selective reactions. For example, substrate size selectivity has been reported as a noteworthy

feature of PCP catalysts.^{2,3} Larger, or bulkier, substrates cannot react in the nanochannels of PCPs, which is accounted for by the channel size and uniformity of the pores. Recently, several groups have successfully performed asymmetric catalytic reactions using chiral porous frameworks,^{2c,4} and the chiral PCP channels have demonstrated their utility in heterogeneous asymmetric reactions, such as transesterification,^{4a} hydrogenation,^{4b,c} and epoxidation.^{4d} In this regard, the ability to incorporate a variety of organic moieties into the nanochannels makes PCPs excellent candidates as nanosized reactors, which contrasts strongly with zeolites or other porous metal–oxide materials. That is to say, the capability for modifying the environment of the PCP pores using organic ligands allows for the tuning of the guest molecular arrangement and serves as a route to tailor the reactions in the channels. The important key to attain this chemistry is the systematic functionalization of the pore surface by introducing various substituents into the organic ligands, where the substituent groups can be preinstalled within precursor

[†] Department of Synthetic Chemistry and Biological Chemistry, Kyoto University.

[‡] PRESTO, JST.

[§] iCeMS, Kyoto University.

- (1) For selected reviews on PCPs and MOFs, see: (a) Férey, G. *Chem. Soc. Rev.* **2008**, *37*, 191. (b) Yaghi, O. M.; O'Keeffe, M.; Ockwig, N. W.; Chae, H. K.; Eddaoudi, M.; Kim, J. *Nature* **2003**, *423*, 705. (c) Kitagawa, S.; Kitaura, R.; Noro, S.-i. *Angew. Chem., Int. Ed.* **2004**, *43*, 2334. (d) Fischer, R. A.; Wöll, C. *Angew. Chem., Int. Ed.* **2008**, *47*, 8164. (e) Bradshaw, D.; Claridge, J. B.; Cussen, E. J.; Prior, T. J.; Rosseinsky, M. J. *Acc. Chem. Res.* **2005**, *38*, 273.
- (2) For recent reviews on PCP catalysis and nanosized reactors, see: (a) Forster, P. M.; Cheetham, A. K. *Top. Catal.* **2003**, *24*, 79. (b) Lee, J. Y.; Farha, O. K.; Roberts, J.; Scheidt, K. A.; Nguyen, S.-B. T.; Hupp, J. T. *Chem. Soc. Rev.* **2009**, *38*, 1450. (c) Ma, L.; Abney, C.; Lin, W. *Chem. Soc. Rev.* **2009**, *38*, 1248. (d) Wang, Z.; Chen, G.; Ding, K. *Chem. Rev.* **2009**, *109*, 322.

- (3) (a) Fujita, M.; Kwon, Y. J.; Washizu, S.; Ogura, K. *J. Am. Chem. Soc.* **1994**, *116*, 1151. (b) Horike, S.; Dinca, M.; Tamaki, K.; Long, J. R. *J. Am. Chem. Soc.* **2008**, *130*, 5854. (c) Dybtsev, D. N.; Nuzhdin, A. L.; Chun, H.; Bryliakov, K. P.; Talsi, E. P.; Fedin, V. P.; Kim, K. *Angew. Chem., Int. Ed.* **2006**, *45*, 916. (d) Xamena, F. X. L. I.; Abad, A.; Corma, A.; Garcia, H. *J. Catal.* **2007**, *250*, 294. (e) Hasegawa, S.; Horike, S.; Matsuda, R.; Furukawa, S.; Kinoshita, Y.; Kitagawa, S. *J. Am. Chem. Soc.* **2007**, *129*, 2607.
- (4) (a) Seo, J. S.; Whang, D.; Lee, H.; Jun, S. I.; Oh, J.; Jeon, Y. J.; Kim, K. *Nature* **2000**, *404*, 982. (b) Wu, C.-D.; Hu, A.; Zhang, L.; Lin, W. *J. Am. Chem. Soc.* **2005**, *127*, 8940. (c) Wu, C. D.; Lin, W. *Angew. Chem., Int. Ed.* **2007**, *46*, 1075. (d) Cho, S.-H.; Ma, B.; Nguyen, S. B. T.; Hupp, J. T.; Albrecht-Schmitt, T. E. *Chem. Commun.* **2006**, 2563.

ligands before PCP synthesis or be postmodified after the formation of the PCPs.⁵ However, alternation of substituents in organic ligands has been studied mainly for tuning the adsorption properties of PCPs,^{5a-e} and few studies have focused on their application to nanoreactors.^{5h} The design of PCPs by tuning the ligands and substituent groups is strongly related to the control of pore characteristics, and such pore engineering will lead to the successful performance of regulating reactions in PCP nanochannels.

The advent of efficient methods for taming radical polymerizations into controlled polymerizations has long been required for the further development of functional polymer materials by tuning primary polymer structures.⁶ However, in conventional processes, the highly reactive free-radical species induce an uncontrolled rapid chain growth without stereoselectivity, and the reaction undergoes inevitable termination via a radical-radical coupling and disproportion. In particular, control of the tacticity in radical polymerization of vinyl monomers is very difficult because of the lack of efficient methods for providing a stereospecific environment around the propagating radical species.⁷ To overcome this problem, many attempts at controlling the tacticity have been carried out by the addition of polar molecules or Lewis acids to the reaction medium.⁸ In such a system, these additives are supposed to interact with vinyl monomers and/or around the propagating radical species to induce a stereospecific chain growth via coordination. A more precise method to control the tacticity is solid-state radical polymerization utilizing nanoporous materials.⁹ Although mesopores (2–50 nm) are too large to regulate vinyl polymerization, microporous hosts (<2 nm) can allow the production of a few stereospecific polymers. Isotactic poly(acrylonitrile) has been prepared in microporous channels composed of urea.^{9d} It should be also noted that polymerization within macromolecularly stereoregular porous thin films provides highly stereoregular vinyl polymers.^{9f} However, in these systems, the effect of

the pores on the stereoregularity of the resulting polymers is still unclear because of the limitation of pore design and versatility. Thus, tailor-made porous matrix design would contribute to the rational control of tacticity in a radical polymerization system.

Tunable microporous PCP channels can be utilized for this strategy.¹⁰ In a previous work, the radical polymerization of vinyl monomers was performed in PCP channels without any substituent groups on the aromatic ligands.¹¹ However, the stereoregularity of the obtained polymers was found to be almost unchanged, and the effect of the PCP nanochannels on the tacticity seemed relatively small. Thus, significant improvement is a prerequisite for regulating the tacticity of a vinyl polymer. Here, we demonstrate a remarkable effect of PCPs on the tacticity of poly(methyl methacrylate) (PMMA), where the introduction of substituents on the organic ligands of the PCPs had a strong influence on the tacticity of PMMA prepared in the channels of $[\text{Cu}_2\text{L}_2(\text{ted})_n]$ (where ted = triethylenediamine and L = monosubstituted terephthalate, **1**; L = 2,5-disubstituted terephthalate, **2**; and L = 2,3-disubstituted terephthalate, **3**). The control of PMMA stereoregularity was accomplished by local and also global design of the PCP channel structure. The appropriate positioning of substituents on the terephthalate moiety resulted in the formation of PCP with a highly regular, very narrow, and helical channel structure, which turned out to be effective for increasing isotacticity of PMMA.

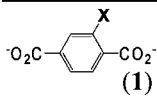
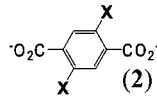
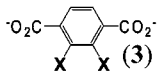
Experimental Section

Materials. All the reagents and chemicals used were obtained from commercial sources, unless otherwise noted. The 2,2'-azobis(isobutyronitrile) (AIBN) was recrystallized from MeOH solution, and the methyl methacrylate (MMA) was purified by vacuum distillation prior to use. Several bridging ligands, such as 2-fluoroterephthalic acid,¹² 2-chloroterephthalic acid,¹³ 2-methoxyterephthalic acid,¹⁴ 2,3-difluoroterephthalic acid,¹⁵ 2,3-dimethoxyterephthalic acid,¹⁶ 2,5-difluoroterephthalic acid,¹⁷ and 2,5-dimethoxyterephthalic acid,¹⁸ were prepared using methods described previously.

Preparation of 2-Methylterephthalic Acid. Anhydrous THF (50 mL) was added to magnesium turnings (0.96 g, 40 mmol) in a

- (5) (a) Devic, T.; Horcajada, P.; Serre, C.; Salles, F.; Maurin, G.; Moulin, B.; Heurtaux, D.; Clet, G.; Vimont, A.; Greneche, J.-M.; Le Ouay, B.; Moreau, F.; Magnier, E.; Filinchuk, Y.; Marrot, J.; Lavalley, J.-C.; Daturi, M.; Férey, G. *J. Am. Chem. Soc.* **2010**, *132*, 1127. (b) Eddaoudi, M.; Kim, J.; Rosi, N.; Vodak, D.; Watcher, J.; O'Keefe, M.; Yaghi, O. M. *Science* **2002**, *295*, 469. (c) Rowsell, J. L. C.; Yaghi, O. M. *J. Am. Chem. Soc.* **2006**, *128*, 1315. (d) Babarao, R.; Jiang, J. *Langmuir* **2008**, *24*, 6270. (e) Tanabe, K. K.; Wang, Z.; Cohen, S. M. *J. Am. Chem. Soc.* **2008**, *130*, 8508. (f) Wang, Z.; Cohen, S. M. *Chem. Soc. Rev.* **2009**, *38*, 1315. (g) Goto, Y.; Sato, H.; Shinkai, S.; Sada, K. *J. Am. Chem. Soc.* **2008**, *130*, 14354. (h) Ingleson, M. J.; Barrio, J. P.; Guilbaud, J. B.; Khimyak, Y. Z.; Rosseinsky, M. J. *Chem. Commun.* **2008**, 2680.
- (6) For representative reviews on controlled or living radical polymerization, see: (a) Moad, G.; Solomon, D. H. *The Chemistry of Radical Polymerization*, 2nd ed.; Elsevier Science: Oxford, UK, 2006. (b) Matyjaszewski, K.; Davis, T. P. *Handbook of Radical Polymerization*; Wiley-Interscience: New York, 2002. (c) Braunecker, W. A.; Matyjaszewski, K. *Prog. Polym. Sci.* **2007**, *32*, 93. (d) Ouchi, M.; Terashima, T.; Sawamoto, M. *Chem. Rev.* **2009**, *109*, 4963. (e) Yamago, S. *Chem. Rev.* **2009**, *109*, 5051. (f) Iha, R. K.; Wooley, K. L.; Nyström, A. M.; Burke, D. J.; Kade, M. J.; Hawker, C. J. *Chem. Rev.* **2009**, *109*, 5620.
- (7) For recent reviews on stereoregulated radical polymerization, see: (a) Satoh, K.; Kamigaito, M. *Chem. Rev.* **2009**, *109*, 5120. (b) Kamigaito, M.; Satoh, K. *Macromolecules* **2008**, *41*, 269. (c) Habaue, S.; Okamoto, Y. *Chem. Rec.* **2001**, *1*, 46.
- (8) (a) Yamada, K.; Nakano, T.; Okamoto, Y. *Macromolecules* **1998**, *31*, 7598. (b) Isobe, Y.; Fujioka, D.; Habaue, S.; Okamoto, Y. *J. Am. Chem. Soc.* **2001**, *123*, 7180. (c) Lutz, J.-F.; Neugebauer, D.; Matyjaszewski, K. *J. Am. Chem. Soc.* **2003**, *125*, 6986. (d) Lutz, J.-F.; Jakubowski, W.; D.; Matyjaszewski, K. *Macromol. Rapid Commun.* **2004**, *25*, 486. (e) Wan, D.; Satoh, K.; Kamigaito, M. *Macromolecules* **2006**, *39*, 6882. (f) Hirano, T.; Miyazaki, T.; Ute, K. *J. Polym. Sci., Part A: Polym. Chem.* **2008**, *46*, 5698.
- (9) (a) Farina, M.; Di Silvestro, G.; Sozzani, P. In *Comprehensive Supramolecular Chemistry*; Reinhoudt, D., Ed.; Pergamon: Oxford, 1996; Vol. 10, p 371. (b) Miyata, M. In *Comprehensive Supramolecular Chemistry*; Reinhoudt, D., Ed.; Pergamon: Oxford, 1996; Vol. 10, p 557. (c) Allcock, H. R.; Silverberg, E. N.; Dudley, G. K. *Macromolecules* **1994**, *27*, 1033. (d) Minagawa, M.; Yamada, H.; Yamaguchi, K.; Yoshii, F. *Macromolecules* **1992**, *25*, 503. (e) Blumstein, A.; Malhotra, A. L.; Watterson, A. C. *J. Polym. Sci. Part A-2* **1970**, *8*, 1599. (f) Serizawa, T.; Hamada, K.-i.; Akashi, M. *Nature* **2004**, *429*, 52.
- (10) (a) Uemura, T.; Yanai, N.; Kitagawa, S. *Chem. Soc. Rev.* **2009**, *38*, 1228. (b) Uemura, T.; Horike, S.; Kitagawa, S. *Chem. Asian J.* **2006**, *1*, 36–44. (c) Vitorino, M. J.; Devic, T.; Tromp, M.; Férey, G.; Visseaux, M. *Macromol. Chem. Phys.* **2009**, *210*, 1923.
- (11) Uemura, T.; Ono, Y.; Kitagawa, K.; Kitagawa, S. *Macromolecules* **2008**, *41*, 87.
- (12) Bernhard, H. G.; Markus, C. G.; Peter, N.; Ulrich, W. S. *Macromol. Chem. Phys.* **2000**, *201*, 1476.
- (13) Shen, H. C.; McDowell, C. C.; Sankar, S. S.; Freeman, B. D.; Kumpf, R. J.; Wicks, D. A.; Lantman, C. W.; Noel, C. *J. Polym. Sci. Part B* **1996**, *34*, 1347.
- (14) Higashi, F.; Nakajima, K.; Zhang, X. *J. Polym. Sci.: Part A* **1994**, *32*, 747.
- (15) Sugawara, S.; Ishikawa, N. *Kogyokagakuzaasshi* **1970**, *74*, 972.
- (16) Crowther, G. P.; Sundberg, R. J.; Sarpeshkar, A. M. *J. Org. Chem.* **1984**, *49*, 4657.
- (17) Huang, X.-S.; Qing, F.-L. *J. Fluorine Chem.* **2008**, *129*, 1076.
- (18) Passaniti, P.; Browne, W. R.; Lynch, F. C.; Hughes, D.; Nieuwenhuyzen, M.; James, P.; Maestri, M.; Vos, J. G. *J. Chem. Soc., Dalton Trans.* **2002**, 1740.

Table 1. Radical Polymerization of MMA in Nanochannels of [Cu₂(L)₂(ted)]_n (1–3) at 70 °C for 9 h

L	X	Amount of MMA			Tacticity (%) ^c		
		(number/unit cell) ^a	Conv. (%) ^a	M _n (M _w /M _n) ^b	mm:mr:rr	ΣP ^d	ρ ^e
 (1)	F	2.7	81	78,700 (3.2)	9:41:50	0.986	1.015
	Cl	2.6	85	93,700 (2.2)	7:41:52	1.028	0.973
	NH ₂	2.6	30	33,100 (1.8)	13:41:46	0.920	1.087
	CH ₃	2.5	51	10,500 (2.3)	8:38:54	0.964	1.037
	Br	2.2	56	50,800 (3.2)	9:41:50	0.986	1.015
	NO ₂	2.2	0	-	-	-	-
	OCH ₃	2.1	53	19,500 (2.3)	13:44:43	0.967	1.034
 (2)	F	2.4	57	39,700 (2.1)	10:45:45	1.026	0.975
	Cl	2.2	66	42,400 (2.1)	11:50:39	1.085	0.922
	CH ₃	2.1	86	32,900 (1.9)	14:48:38	1.019	0.982
	Br	2.1	28	4,300 (1.3)	19:46:35	0.944	1.059
	OCH ₃	1.9	42	37,100 (2.0)	28:53:19	1.069	0.936
 (3)	F	2.7	64	24,500 (2.2)	8:40:52	0.992	1.008
	OCH ₃	1.9	81	12,900 (2.9)	8:39:53	0.978	1.022
Bulk polym. ^f	-	-	-	56,100 (6.4)	5:35:60	1.004	0.996

^a Determined by TGA. ^b Obtained by GPC calibrated by PMMA standards. ^c Determined by ¹H NMR measurement in nitrobenzene-*d*₅ at 110 °C. ^d ΣP = P_{mr} + P_{rm}, where P_{mr} = [mr]/(2[mm] + [mr]) and P_{rm} = [mr]/(2[rr] + [mr]). ^e ρ = 2[m][r]/[mr]. ^f Bulk polymerization was carried out under a comparable condition to those employed in PCPs.

100 mL three-neck flask under a nitrogen atmosphere. After addition of 2,5-dibromotoluene (1.99 g, 8 mmol), the mixture was heated to 60 °C, and then 1,2-dibromoethane (3.30 g, 18 mmol) was added to activate the magnesium metal. The resulting mixture was stirred for a period of 15 h at 60 °C and cooled to -78 °C. An excess amount of dry ice was added to the reaction mixture, and the mixture was allowed to reach room temperature and then stirred for 3 h. The reaction was quenched with a 3 N aqueous solution of HCl (20 mL) and extracted with diethyl ether (20 mL). The organic layer was washed with water several times and dried over Na₂SO₄. The solvent was removed, and the white powder product was dried in a vacuum (1.20 g, 83%). ¹H NMR (DMSO-*d*₆): δ = 2.55 (s, 3H), δ = 7.77–7.87 (m, 3H).

Preparation of 1–3. These porous compounds were prepared according to reported preparation methods.¹⁹ Solutions of terephthalic acids (6.4 mmol) in DMF or MeOH (300 mL) were slowly added to a methanol solution (50 mL) containing CuSO₄·5H₂O (1.6 g, 6.4 mmol). After being stirred for 3 days at room temperature, the resultant blue precipitate was collected by centrifugation and transferred to a stainless sealed Teflon reaction vessel. After the addition of DMF (30 mL), a toluene solution (20 mL) of ted (0.36 g, 3.2 mmol) was then added to the vessel. The mixture was allowed to react at 140 °C for 6 h, and then the resultant precipitates was filtered, washed with MeOH, and dried under reduced pressure.

Polymerization of MMA in 1–3. The dried host compound (50 mg) was prepared by evacuation (<0.1 kPa) at 130 °C for 5 h in a Pyrex reaction tube. Subsequently, the host powder was immersed in MMA (0.13 mL) with AIBN (1 mg) at room temperature for 0.5 h to incorporate MMA and the radical initiator into the nanochannels. After excess monomer external to the host crystals was removed completely by evacuation (2.0 kPa) at room temperature for 1 h, the reaction tube was filled with nitrogen and heated to 70 °C to perform the polymerization over a period of 9 h. After the polymerization was complete, the composite was washed with MeOH to remove any unreacted MMA. To isolate

Table 2. Temperature Effects on Polymerization of MMA in 2OMe

reaction temp ^a (°C)	reaction time (h)	conv ^{b,c} (%)	tacticity ^d mm:mr:rr
90	9	48	26:59:16
70	9	42	28:53:19
60	9	65	23:55:22
50	9	63	24:54:22
20	48	n.d.	24:46:30
3	96	n.d.	24:47:29
-20	96	23	25:50:25
-40	96	21	23:56:21
-78	168	0	

^a Low-temperature polymerizations below 20 °C were initiated with tributylborane–oxygen system. ^b Determined by TGA. ^c n.d. = not determined. ^d Determined by ¹H NMR measurement in nitrobenzene-*d*₅ at 110 °C.

the PMMA inside the channels, the composite was stirred in a 0.05 M aqueous solution (15 mL) of sodium ethylenediaminetetraacetate (Na–EDTA) for 3 h for the complete dissolution of the host porous framework. The collected polymer product was washed with water (2 mL × 3) and dried under a reduced pressure at room temperature.

The amount of monomer MMA adsorbed in the PCPs without AIBN was calculated from the weight loss up to 200 °C by thermogravimetric analysis (TGA), as shown in Table 1. We compared the value of the weight loss corresponding to the adsorbed MMA in the PCPs before and after polymerization to determine the monomer conversion rate (Table 1 and 2). Quantitative recovery of the resulting PMMA was confirmed after the dissolution of PCP frameworks by comparison with the conversion ratio.

Polymerization of MMA below 20 °C. The dried powder of 2 composed of 2,5-dimethoxyterephthalate (2OMe; 50 mg) was immersed in a mixture of Et₂O (170 μL), MMA (80 μL), and a 1.0 M Et₂O solution of tributylborane (10 μL) for 20 min at room temperature in a nitrogen atmosphere. The Et₂O was evacuated at 20 kPa for 10 min, followed by removal of any excess MMA at 2.0 kPa for 0.5 h. Then, the reaction vessel was filled with nitrogen and cooled to the appropriate temperature. The polymerization of the MMA was initiated using oxygen by inletting air using a microsyringe. To quench the polymerization, a 10 wt % MeOH solution of di-*tert*-butylcresol (3 mL) was added, and the resulting

(19) (a) Seki, K.; Mori, W. *J. Phys. Chem. B* **2002**, *106*, 1380. (b) Kitaura, R.; Iwahori, F.; Matsuda, R.; Kitagawa, S.; Kubota, Y.; Takata, M.; Kobayashi, T. *C. Inorg. Chem.* **2004**, *43*, 6522. (c) Matsuda, R.; Kitaura, R.; Kitagawa, S.; Kubota, Y.; Takata, M. To be submitted.

composite was washed with MeOH (3 mL \times 2). Isolation of the encapsulated PMMA was performed in an aqueous Na–EDTA solution using the method discussed above.

Molecular Dynamics Simulation. Molecular dynamics (MD) simulations of the PCPs were performed using the Materials Studio Modeling v4.4 software package (Accelrys Inc., San Diego, CA) using the Universal Force Field,²⁰ as implemented in the *Forcite* module. The charges were dealt with by charge equilibration method in this system. The initial structures of the PCPs were generated on the basis of the X-ray crystal structures. The quench dynamics with the optimized structures were conducted at 3000 K, and then MD calculations were carried out at 300 K for 200 ps under NVT conditions.

Measurements. The X-ray powder diffraction (XRPD) data were collected using a Rigaku RINT 2000 Ultima diffractometer employing Cu K α radiation. The TGA was carried out from room temperature to 500 °C at a heating rate of 10 °C min⁻¹ using a Rigaku Instrument Thermo plus TG 8120 in a nitrogen atmosphere. Nitrogen adsorption measurements at 77 K were carried out using a Quantachrome Autosorb-1. The samples were dried under high vacuum (<10⁻² Pa) at 120 °C for 5 h before the measurements were performed. The Dubinin–Radushkevich (DR) equation was used to characterize the detailed porous properties of the PCPs.²¹ The DR equation is given by

$$\ln W = \ln W_0 + (A/\beta E_0)^2$$

where W and W_0 are the amount of nitrogen adsorbed at a relative pressure (P/P_0) and the saturated amount of nitrogen adsorbed, respectively, E_0 is a characteristic adsorption energy, and the parameter A is Polanyi's adsorption potential, defined as $A = RT \ln(P_0/P)$. The parameter β is the affinity coefficient and is related to the adsorbate–adsorbent interaction. The DR plots showed a linear relationship in the lower P_0/P region, from which the micropore volume and the value of βE_0 were obtained. The micropore volume, V_m , was calculated from the value of W_0 and the density of liquid nitrogen at 77 K (0.807 g cm⁻³). The ¹H and ¹³C NMR spectra were obtained using a JEOL A-500 spectrometer operating at 500 MHz. The GPC measurements on the PMMA were performed in CHCl₃ at 40 °C on three linear-type polystyrene gel columns (Shodex K-805 L) that were connected to a JASCO PU-980 precision pump, a JASCO RI-930 refractive index detector, and a JASCO UV-970 UV/vis detector set at 256 nm. The columns were calibrated against standard PMMA samples. The infrared spectra were measured using KBr disks employing a Perkin-Elmer Spectrum BX FT-IR system.

Results and Discussion

Preparation of Host PCPs. Most of the host compounds **1–3** were newly prepared by heating a mixture of Cu²⁺, ted, and the various types (mono-, 2,5-di-, and 2,3-disubstitution) of terephthalate ligands in sealed vessels (Figure 1).¹⁹ XRPD measurements on **1–3** gave diffraction patterns characteristic of the previously reported [Cu₂(terephthalate)₂(ted)]_n (Figure 2),^{11,19a} which reveals that layered structures based on Cu²⁺ and terephthalates are linked with ted as a pillar ligand and one-dimensional microporous channels are formed along the pillar ligand (Figure 1). The microporous structure of **1–3** was confirmed by nitrogen adsorption measurement, which showed Type I isotherms for all the samples, and the size of the pores was ca. 4–7 Å. TGA of the host compounds **1–3** fully

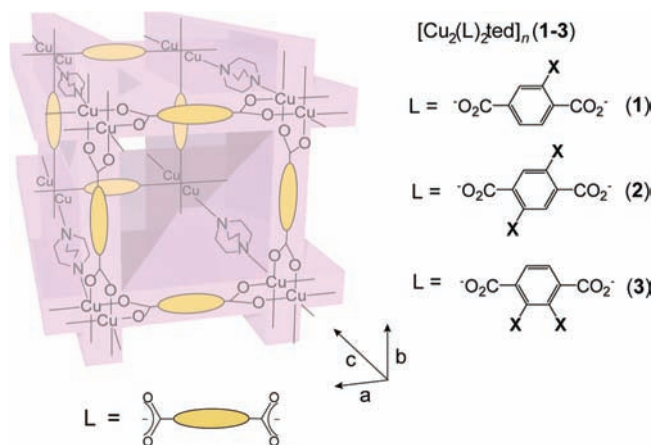


Figure 1. Schematic illustration of [Cu₂(L)₂(ted)]_n (**1–3**).

encapsulating MMA in the nanochannels exhibited a weight loss corresponding to the adsorbed MMA up to 200 °C, also suggesting a nanoporous structure was present in **1–3**. From these analyses, a correlation between the amount of adsorbed guest molecules and the pore size of **1–3** was clearly seen, where the adsorption amount decreased with increasing number or size of the substituent on the terephthalate (Table 1).

Radical Polymerization of MMA in PCPs. Considering the size of MMA (molecular size = 5.9 \times 4.1 Å), only single chains of PMMA can propagate in the channels of the PCPs, and thus, the pore walls of the PCPs will strongly influence the polymerization. Radical polymerization of MMA in the channels of **1** with monosubstituted terephthalates was carried out as follows. The MMA monomer was adsorbed in the channels by immersion of **1** in MMA, followed by removal of any excess MMA external to the host crystals under reduced pressure. The host–monomer inclusion compounds were then heated with AIBN to induce polymerization at 70 °C for 9 h. No change in the peak patterns was observed in the XRPD profiles of **1** during the polymerization, indicating that the channel structures of **1** were maintained on the inclusion and polymerization of MMA. The resulting PMMA was quantitatively recovered from the composites by dissolution of the frameworks of **1** in an aqueous Na–EDTA solution. Table 1 summarizes the polymerization results (conversion, molecular weight, and tacticity) of MMA in the nanochannels of **1**. The polymerization proceeded in good yields, except for the case of using **1** with a nitro-substituted ligand. This is because the generated radical was quenched by the nitro group on the pore walls.²² From the viewpoint of tacticity, the ¹H NMR spectrum of the resulting PMMA was measured to determine the triad fractions corresponding to the methyl groups on the main chain.²³ In these measurements, the nanochannels of **1** were found to produce PMMA with more isotactic and heterotactic triads compared with conventional bulk and solution polymerizations (Table 1). Radical polymerization of MMA using the channels of [Cu₂(terephthalate)₂(ted)]_n (a nonsubstituted terephthalate) provided PMMA with a triad tacticity mm:mr:rr = 8:40:52.¹¹ Thus, a measurable effect of the substituent group on the stereoregularity of PMMA was confirmed; in particular, the use of terephthalate ligands with amino and methoxy substituents showed relatively large influences on tacticity (Table 1 and Figure 3).

Next, we performed polymerization of MMA utilizing the channels of **2** consisting of 2,5-disubstituted terephthalates for

(20) (a) Rappé, A. K.; Casewit, C. J.; Colwell, K. S.; Goddard, W. A., III; Skiff, W. M. *J. Am. Chem. Soc.* **1992**, *114*, 10024. (b) Casewit, C. J.; Colwell, K. S.; Rappé, A. K. *J. Am. Chem. Soc.* **1992**, *114*, 10035. (c) Casewit, C. J.; Colwell, K. S.; Rappé, A. K. *J. Am. Chem. Soc.* **1992**, *114*, 10046.

(21) Dubinin, M. M. *Chem. Rev.* **1960**, *60*, 235.

(22) Bovey, F. A.; Kolthoff, I. M. *Chem. Rev.* **1948**, *42*, 491.

(23) Hatada, K. *J. Polym. Sci., Part A: Polym. Chem.* **1999**, *37*, 245.

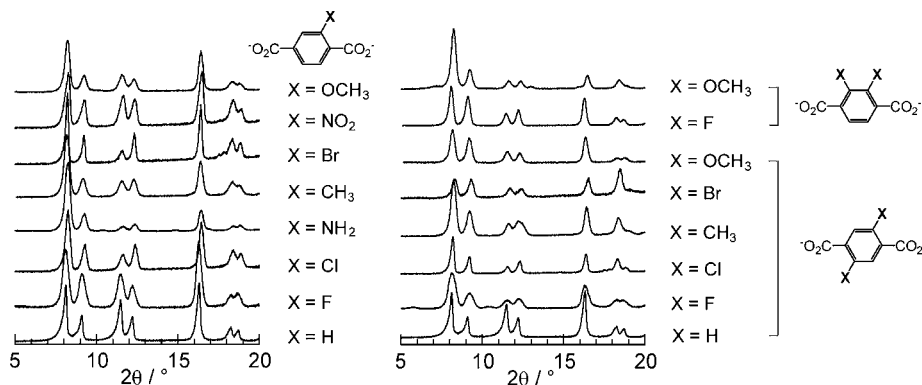


Figure 2. XRPD patterns of $[\text{Cu}_2(\text{L})_2(\text{ted})]_n$ (**1–3** and L = terephthalate).

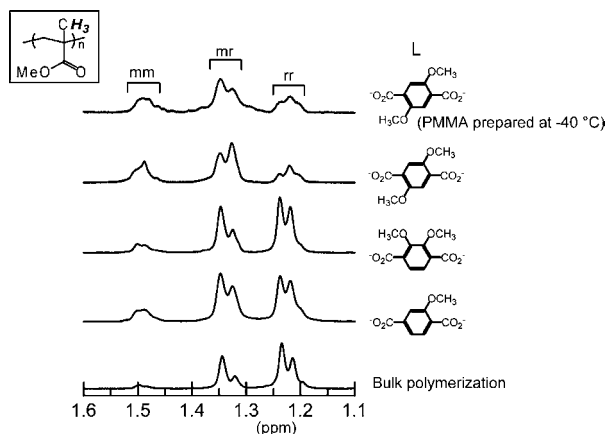


Figure 3. ^1H NMR spectra of PMMA in nitrobenzene- d_5 at $110\text{ }^\circ\text{C}$ prepared in the bulk condition and in the nanochannels of $[\text{Cu}_2(\text{L})_2\text{ted}]_n$ (L = methoxy-substituted ligands). The polymerizations were carried out at $70\text{ }^\circ\text{C}$ unless otherwise noted.

further change of the tacticity of PMMA (Table 1). Although PMMA could be prepared in all the channels, the yield and molecular weight of the obtained polymer were relatively low in the case of using **2** with a bromo-substituted ligand, which was probably because of the low crystallinity of the host (Figure 2). A marked effect of the substitution groups on the stereoregularity of the PMMA was observed in this polymerization system, revealing that additional attachments of the substituents lead to an increase in the mm and mr fractions of PMMA compared with those prepared in **1** composed of corresponding monosubstituted terephthalates (Table 1). Interestingly, this effect became more obvious as the substituent group on the terephthalate in **2** was larger. The use of a larger substituent fills the pore space, resulting in a narrower channel structure. Such narrow channels induce polymerization with less sterically bulky isotactic units rather than syndiotactic units.^{11,24} When we polymerized MMA in **2** with 2,5-dimethoxyterephthalate (**2OMe**), PMMA with high mm and mr contents (mm:mr:rr = 28:53:19) was obtained (Table 1 and Figure 3). This change of PMMA tacticity is much larger than those previously reported in controlled radical polymerization systems, and thus, the utilization of this porous framework is one of the most effective methods for changing tacticity in radical polymerization of MMA.^{9e,f}

To study the details of the effect of substituent, several PCPs with 2,3-disubstituted groups (**3**) were prepared and used in the polymerization of MMA (Table 1). In contrast to the polymerization in **2**, syndiotacticity of the PMMA obtained in **3** increased in comparison with those prepared in the corresponding channels of **1**. Note that the triad tacticities of PMMA obtained in **3** with 2,3-dimethoxyterephthalate (**3OMe**) (mm:mr:rr = 8:39:53) were almost the same to those obtained for nonsubstituted $[\text{Cu}_2(\text{terephthalate})_2\text{ted}]_n$ (Figure 3).¹¹ This result clearly suggests that the tacticity of PMMA synthesized in PCPs strongly depends on the position of substituents on the ligands.

Detailed Analysis of the Polymerization. The interaction between MMA and the pore walls of the PCPs was examined using IR spectroscopy. The IR spectrum of neat MMA shows a strong band corresponding to the C=O stretching occurring at 1726 cm^{-1} . Similarly, the peak from the C=O moiety of MMA appears at $1720\text{--}1729\text{ cm}^{-1}$ in all the spectra of PCP–MMA inclusion compounds, and the peak position is independent of the host structures of **1–3**. In addition, the peaks of the MMA unit do not shift after the polymerization of MMA in the channels of **1–3**. Thus, these results rule out the possibility that the stereoregularity of PMMA is affected by a strong interaction between MMA and the channel walls of the PCPs.

In vinyl polymer systems, when stereoregulation in the addition of monomers to propagating radicals is not influenced by the stereostructure of all the other placements, then the distribution of tacticity obeys the theory of Bernoulli statistics.²⁵ Previous NMR analysis has indicated that Bernoulli statistics can be applied to the radical polymerization of MMA at $70\text{ }^\circ\text{C}$.²⁶ To examine the effect of PMMA tacticity on the resulting stereosequence during the polymerization in PCPs, we calculated the important parameters using the following relationships:

$$P_{m/r} = 1 - P_{m/m} = [\text{mr}]/(2[\text{mm}] + [\text{mr}])$$

$$P_{r/m} = 1 - P_{r/r} = [\text{mr}]/(2[\text{rr}] + [\text{mr}])$$

where $P_{m/r}$ is the probability that a racemo addition follows a meso addition, $P_{r/m}$ is the probability that a meso addition follows a racemo addition, and $[\text{mm}]$, $[\text{mr}]$, and $[\text{rr}]$ are the

- (25) (a) Coleman, B. D.; Fox, T. G. *J. Polym. Sci. Part A* **1963**, *1*, 3183. (b) Hatada, K.; Kitayama, T.; Ute, K. *Prog. Polym. Sci.* **1988**, *13*, 189. (c) Tanaka, Y.; Yamaguchi, F.; Shiraki, M.; Okada, A. *J. Polym. Sci.: Polym. Chem. Ed.* **1978**, *16*, 1027. (26) Bovey, F. A.; Tires, G. V. D. *J. Polym. Sci.* **1960**, *44*, 173.

(24) Hunt, M. A.; Shamsheer, J. M.; Uyar, T.; Tonelli, A. E. *Polymer* **2004**, *45*, 1345.

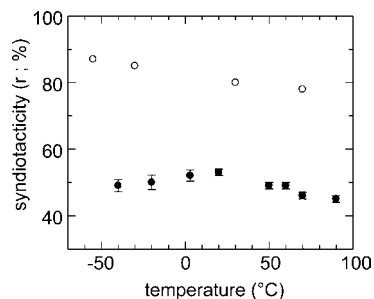


Figure 4. Effect of polymerization temperature on syndiotacticity of PMMA prepared in **2OMe** (filled circle) and under bulk conditions^{25b,27} (open circle).

observed triad fractions. If stereoregulation follows Bernoullian statistics, then

$$P_{m/m} = P_{r/m} = P_m$$

$$P_{r/r} = P_{m/r} = P_r$$

and thus

$$\Sigma P = P_{m/r} + P_{r/m} = 1$$

where P_m and P_r are the fractions of meso and racemo diads, respectively. The value of ΣP obtained in the case of bulk polymerization is almost equal to unity, supporting a Bernoullian pathway.²⁶ However, the results of the analysis of our polymerization studies show that the tacticity of PMMA prepared in PCP channels slightly deviates from Bernoullian theory (Table 1). In particular, it seems that PMMA with lower syndiotacticity shows a larger deviation, suggesting that the addition of the monomer was influenced by the stereochemistry of the growing chain ends in those systems.²⁵ To study the details of the polymerization mechanism, the Coleman–Fox parameter,^{25a} which is defined in the equation below, was calculated from the tacticity values of the PMMA.

$$\rho = 2[m][r]/[mr]$$

The value of ρ for the polymers obtained in our experiments was found to be equal to $(\Sigma P)^{-1}$ (Table 1), which means that the polymerization of MMA in the PCP channels can be described using first-order Markov statistics.²⁵ Thus, this fact clearly demonstrates that there is a penultimate effect in the stereoregulation of the polymerization in the PCP nanochannels.

Using the nanochannels of **2OMe**, the effect of the polymerization temperature on the tacticity of PMMA was studied from -78 to 90 °C (Table 2 and Figure 4). In the usual polymerization of MMA in solution or in the bulk state, syndiotacticity of PMMA continuously increases with decreasing reaction temperature (Figure 4).^{25b,27} In contrast, the syndiotacticity of PMMA prepared in **2OMe** once increased slightly, and then became lower, as the reaction temperature decreased. Thus, PMMA obtained at lower temperatures still contained high mm and mr triad fractions. This unique phenomenon is ascribable to the suppressed mobility (vibration and rotation) of the PCP framework at lower temperatures. Such quiescent channels would ef-

Table 3. Micropore and Thermodynamic Parameters of **2OMe** and **3OMe**

	W_0 (cm ³ /g)	V_m (cm ³ /g)	βE_0 (kJ/mol)
2OMe	297	0.46	10.0
3OMe	294	0.46	9.7

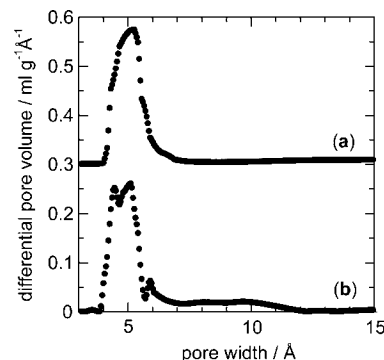


Figure 5. Pore-size distributions of (a) **2OMe** and (b) **3OMe** based on HK model.

fectively control the arrangement of encapsulated MMA, resulting in the large tacticity change of PMMA.

Structural Analysis of **2** and **3** with Dimethoxyterephthalates.

To understand the cause of the different tacticity values of PMMA obtained from the channels of **2** and **3**, we carried out nitrogen adsorption measurements on **2OMe** and **3OMe** at 77 K to elucidate the pore characteristics. As expected from the crystal structures, these PCP compounds exhibited Type I adsorption isotherms, showing a microporous structure. Dubinin–Radushkevich (DR) analysis of the obtained isotherms afforded the saturated amount of adsorption (W_0), micropore volume (V_m), and isosteric heat of adsorption (βE_0).²¹ Table 3 summarizes the micropore and thermodynamic parameters of **2OMe** and **3OMe**, in which no obvious difference in the parameters between **2OMe** and **3OMe** suggests similar micropore dimensions and surface interactions. However, the pore-size distributions of **2OMe** and **3OMe**, calculated using the Horvath–Kawazoe (HK) model,²⁸ showed a critical difference in the pore regularity (Figure 5). The profile of **2OMe** was almost unimodal, with a peak occurring at 5.2 Å; however, several peaks and a broad distribution from 4 to 11 Å were clearly observed in the profile of **3OMe**.

Usually, X-ray analysis is the most powerful methods for determining the crystal structures of PCPs. However, in the case of **2OMe** and **3OMe**, the experimental X-ray structures showed a disordered form of the ligand-rotational isomers, and no distinct structural difference between **2OMe** and **3OMe** was observed. To overcome this problem, we performed MD simulations to determine the global minimum structures of **2OMe** and **3OMe**. Molecular simulation is a useful tool to screen PCP structures for specific applications.²⁹ In particular, accurate MD calculations are helpful in interpreting the ambiguous results from the X-ray analysis and to determine plausible structures of the PCPs.³⁰ Figure 6 shows typical MD structures for **2OMe** and **3OMe**. From our MD simulations, we could

(28) Horvath, G.; Kawazoe, K. *J. Chem. Eng. Jpn.* **1983**, *16*, 470.

(29) (a) Düren, T.; Bae, Y.-S.; Snurr, R. Q. *Chem. Soc. Rev.* **2009**, *38*, 1237. (b) Keskin, S.; Liu, J.; Rankin, R. B.; Johnson, J. K.; Sholl, D. S. *Int. Eng. Chem. Res.* **2009**, *48*, 2355.

(30) Amirjalayer, S.; Schmid, R. *J. Phys. Chem. C* **2008**, *112*, 14980.

(27) Reinmüller, M.; Fox, T. G. *Polym. Prepr., Am. Chem. Soc. Div. Polym. Chem.* **1966**, *7*, 999.

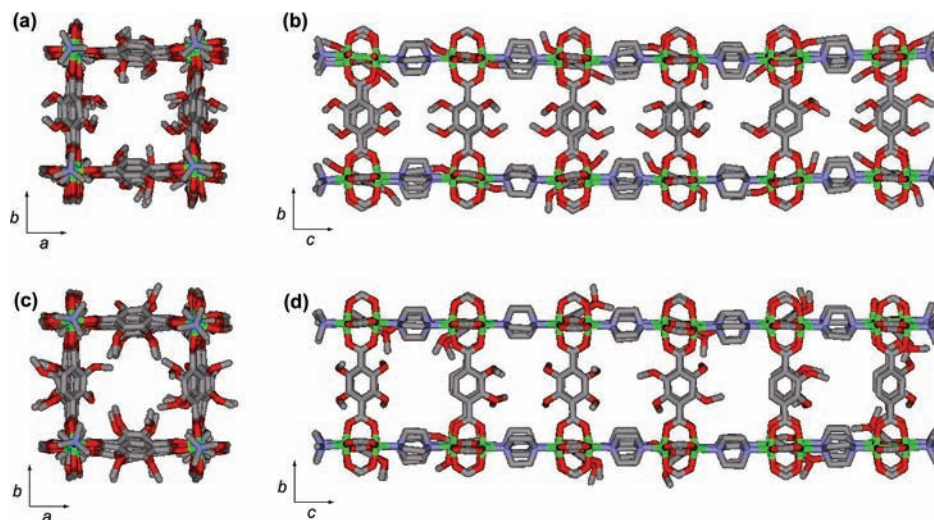


Figure 6. Typical MD structures of (a and b) **2OMe** and (c and d) **3OMe** (Cu, green; O, red; N, blue; C, gray). Hydrogen atoms are omitted for clarity. The series of calculations was performed three times, and the nearly identical structures of **2OMe** and **3OMe** were reproducibly obtained.

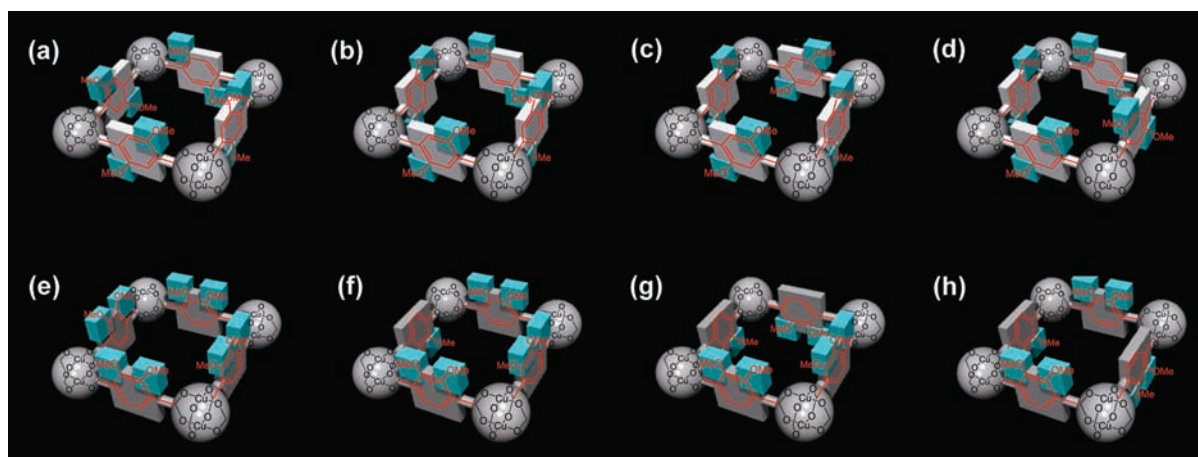


Figure 7. Schematic images of possible rotational isomers of (a–d) **2OMe** and (e–h) **3OMe**.

understand how the global structures of the PCP materials were arranged as a consequence of the local interactions among the substituents on ligands. **2OMe** and **3OMe** have four possible isomers because of the ability of the ligand rotation (Figure 7). Our MD simulations suggest that more than 80% of the unit structures of **2OMe** form the highly regular and symmetrical structure shown in Figure 7a. In contrast, the four rotational isomers (Figure 7e–h) randomly and equivalently exist in the MD structure of **3OMe**, resulting in an irregular channel structure. This different regularity of the PCP pores for **2OMe** and **3OMe** is also supported by the pore size distribution data based on the N_2 adsorption measurements. In this conformational study, it should be also noted that the most plausible rotational isomer of **2OMe** (Figure 7a) forms a helically twisted channel in the framework. Usually, isotactic vinyl polymers prefer helical conformations owing to the steric effects of the side chains.³¹ For example, radical polymerization of methacrylates with large substituent groups produces highly isotactic polymers that form

rigid helices.³² This helical conformation forces the monomer addition to be more and more favorable for isotactic chain propagation, resulting in a deviation from Bernoullian statistics and satisfying the first-order Markov model.^{25b,32a} Because polymerization in the channels of **2OMe** is explained using first-order Markov statistics, the increase of isotacticity of PMMA obtained in the channels would be caused by the regular, narrow, and helical natures of the **2OMe** pores. A previous report has shown that the ligand of $[Zn_2L_2(\text{ted})]_n$ ($L = 1,4\text{-naphthalenedicarboxylate}$) does not freely rotate in the framework, and the rotational motion is considerably decelerated by guest adsorption.³³ Thus, our results here strongly suggest that the appropriate positioning of the substituent groups in the PCP is of utmost importance for determining and tuning PCP systems for practical applications.

Conclusions

In this work, we have prepared a variety of $[Cu_2L_2(\text{ted})]_n$ compounds (**1–3**) by introducing substituent groups into the

(31) (a) Natta, G.; Danusso, F.; Moraglio, G. *Makromol. Chem.* **1958**, *28*, 166. (b) Ashby, G. E.; Hoeg, D. F. *J. Polym. Sci.* **1959**, *39*, 535. (c) Cojazzi, G.; Malta, V.; Celotti, G.; Zannetti, R. *Makromol. Chem.* **1976**, *177*, 915.

(32) (a) Yuki, H.; Hatada, K.; Nishimori, T.; Kikuchi, Y. *Polym. J.* **1970**, *1*, 36. (b) Nakano, T.; Mori, M.; Okamoto, Y. *Macromolecules* **1993**, *26*, 867.

(33) Horike, S.; Matsuda, R.; Tanaka, D.; Matsubara, S.; Mizuno, M.; Endo, K.; Kitagawa, S. *Angew. Chem., Int. Ed.* **2006**, *45*, 7226.

organic ligand L. The ability of surface functionalization by the substituents is one of the most advantageous features of PCPs, and thus, the control of tacticity in radical polymerization of MMA could be attained using the nanochannels of **1–3**. We found that the tacticity of the resulting PMMA strongly depended on the number and position of the substituent, and we have demonstrated the remarkable effect of the PCP pores on the tacticity of PMMA by experimental and theoretical analysis. Note that tacticity of PMMA drastically changed using **2OMe** because of the specific channel shape (regular, narrow, and helically twisted channel) of **2OMe**. Application of PCPs to nanocatalysts or nanoreactors for inducing highly selective reactions is currently attracting much attention but is still in its infancy. We believe that our method presented here will contribute to the tailor-made synthesis of polymer materials owing to the ability to design the pores.

Acknowledgment. We thank Prof. R. Schmid (Ruhr-Universität Bochum) for his helpful advice and discussions on MD simulations. This work was supported by PRESTO-JST and a Grant-in-Aid from the Ministry of Education, Culture, Sports, Science and Technology, Government of Japan.

Note Added after ASAP Publication. An incorrect reference citation appeared in the first paragraph in the version published ASAP March 12, 2010. The corrected version was published March 17, 2010.

Supporting Information Available: X-ray crystal structures, IR, and NMR spectra. This material is available free of charge via the Internet at <http://pubs.acs.org>.

JA100406K